1. Three-dimensional printed sample holder

The novel sample holder designed and 3D-printed for this study is depicted in Figure S1. The sample holders were printed on a commercial Ultimaker S5 fused filament fabrication (FFF) 3D printer using a 0.8 mm nozzle in clear polylactide (natural PLA, purchased from Ultimaker BV). The printing of 10 sample holders takes approx. 1 h and requires 29 g of PLA. The cost of one sample holder (material and running cost of printer) is estimated to be EUR 0.10.

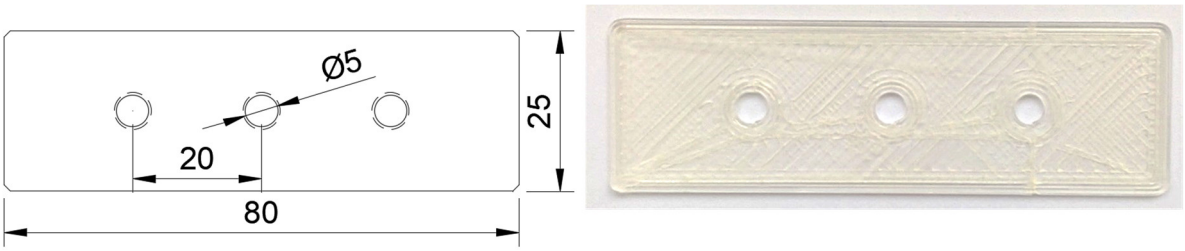

Figure S1. Left: Schematic of the novel transmission IR microscopy sample holder (dimensions in mm). Right: Image of the sample holder, printed in clear (natural) PLA.

Figure S2 shows a sample holder with paraffin sections applied. The sections are "fished" out from the surface of the water of the collection basin and are thus perfectly planar. The application onto the sample holders does not seem to interfere with the integrity of the paraffin, and the rough surface of the 3D-printed material aids with adhesion. The paraffin appears to remain stretched out over the 5 mm aperture for several months of storage at room temperature.

Figure S2. Sample holder (printed in blue PLA for the purpose of this visualization) with paraffin sections applied to two holes.

2. Data acquisition and processing

It is important to note that the physical resolution of the measurement is 10 × 10 µm. In this 100 µm² square, a full IR spectrum is acquired for approx. 4 min (256 integrations), before the sample is moved by precisely 10 µm and the next spectrum is acquired. Thus, there is no overlap in the location of where the spectra are taken. The sampling process is sketched in Figure S3.

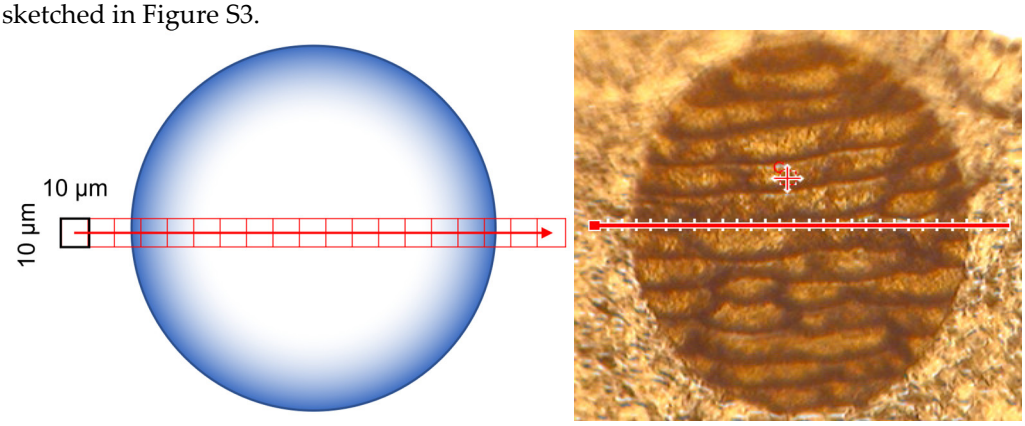

Figure S3. Left: Sketch of the sampling process on ECR1030M. The enzyme distribution is represented by the fading blue color, the IR microscope sampling area by the red squares (not to scale). Right: Light microscopic image of bead section taken prior to IR microscopic sampling. The image, taken by the same device but in visible-light mode, is slightly distorted because the optics are optimized for IR radiation. The sampling squares are not visualized, only the path as indicated by the red arrow.

Figure S4 serves to illustrate that each measurement point along the diameter of the particle represents the IR absorbance of the sample averaged over a 100 µm² area. If the edge of the resin particle happens to be exactly in the middle of a 10 µm × 10 µm square, the measured absorbance at the absorbance band is halved because of the averaging effect between the paraffin and the particle.

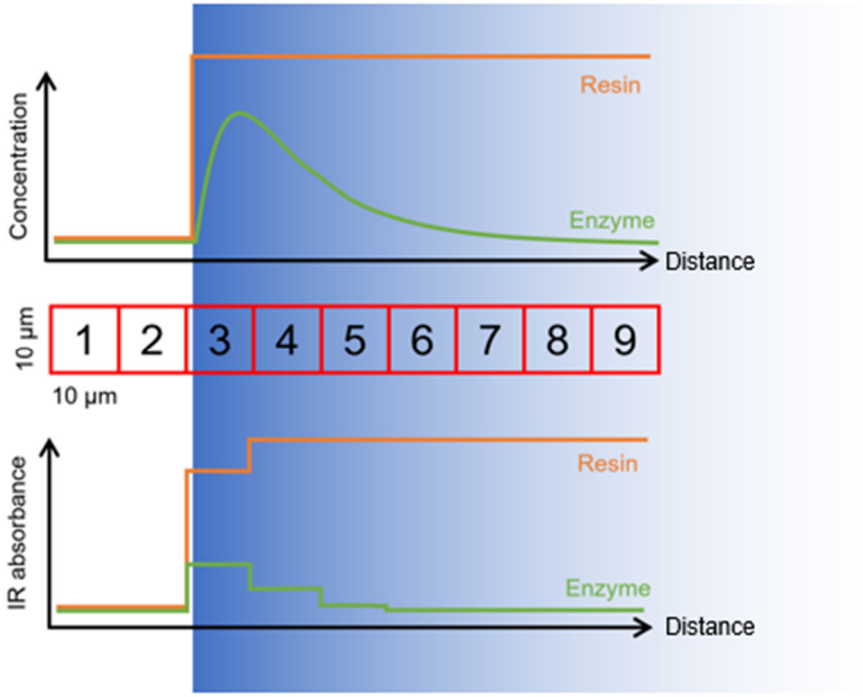

Figure S4. Close-up of the sampling process. The edge of the particle is represented by the vertical blue line. The actual concentration and measured IR absorbance for resin (orange line) and enzyme (green line) are plotted above and below the representation of the acquired spectra (red squares).

To express the penetration characteristics of CalB in one number, namely the penetration depth, an important assumption must be made: an absorbance threshold (or limit) must be defined, above which the enzyme is considered present, and below which the enzyme is considered absent. This is depicted in Figure S5. In the present study, the full width at maximum height (FWMH) was used, meaning the threshold was set at 50% of the signal height. Interpolation was done using a polynominal fit with a high degree of freedom (f = 20) to properly follow the sharp curve of the absorbance.

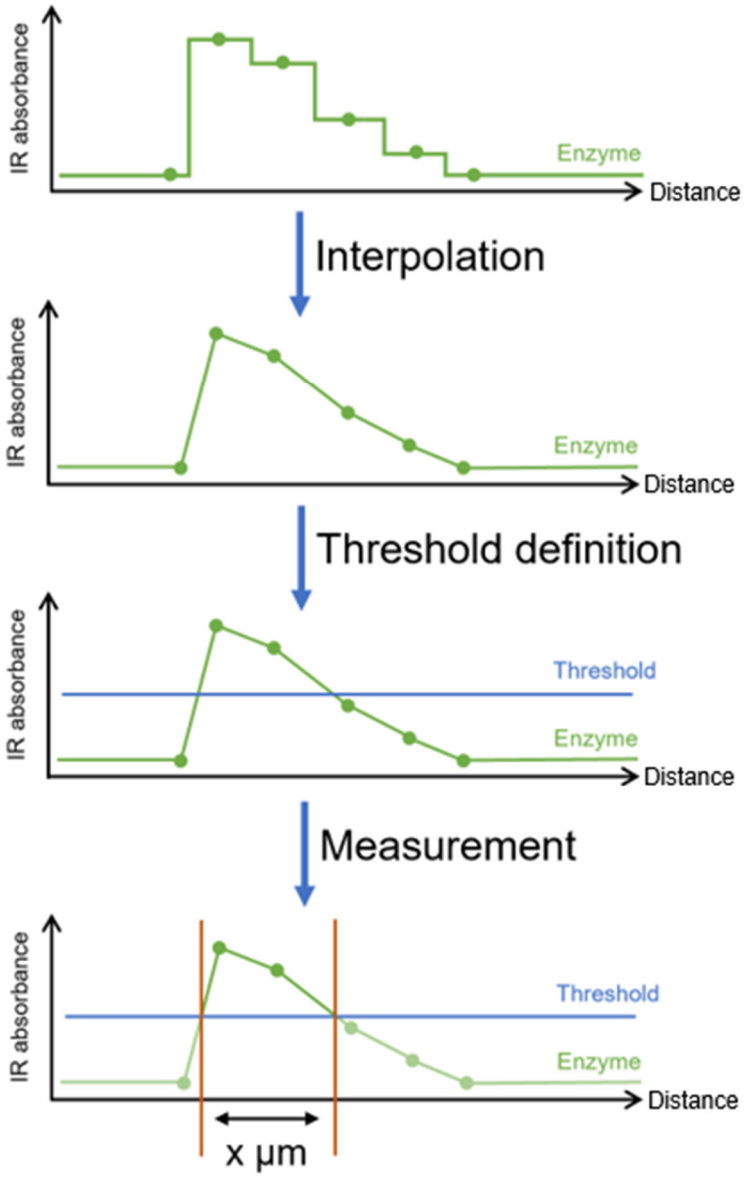

Figure S5. Simplified schematic of data processing for penetration-depth measurements.

3. Representative IR Spectra

Figure S6 shows representative spectra, overlaid to highlight the absorbance at the amide I band (enzyme) and C=O ester (resin). In the middle of the particle, the signal of the resin can still be seen, while the enzyme seems to be completely absent. The height difference of the background (compared to paraffin) is corrected by the single-point baseline taken at 1800 cm^{-1}.

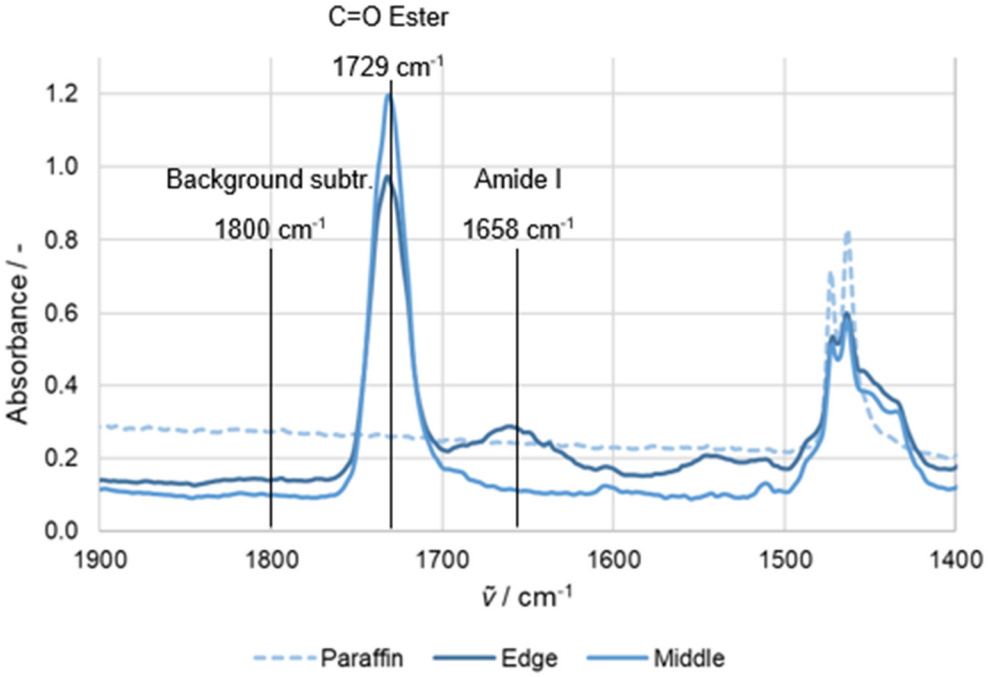

Figure S6. Representative spectra (ECR1030M, 1 h) from the surrounding paraffin and the edge and middle of the sectioned bead.

4. Penetration-depth bias caused by Z-location of the section

The paraffin slices are cut at a thickness of 10 µm. In theory, a particle with a diameter of 500 µm can thus be cut into 50 slices. To calculate the enzyme penetration depth, only the paraffin slice closest to the middle of the particle (the equator) should be used, to minimize the geometrical bias. Figure S7 is a graphical representation of the problem. The apparent penetration depth of the enzyme l_{Enzyme} and the apparent radius of the section $r_{Section}$ change depending on the cutting height (or Z-height) h. The farther the cut is from the equatorial plane, the stronger the penetration depth is overestimated, and the diameter underestimated.

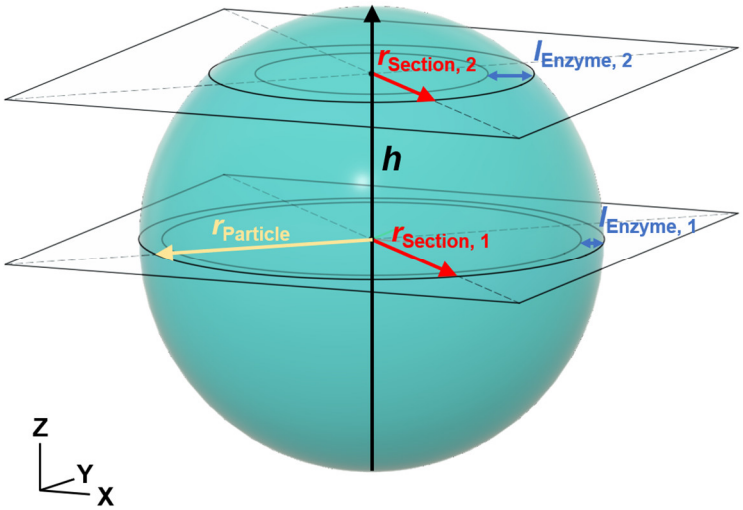

Figure S7. Sketch of a particle sliced exactly through its equator (1) and higher (2).

Three scenarios were calculated, the results of which are presented in Table S1. Considering the resolution of the IR-microscope (10 µm × 10 µm), the geometrically increased penetration depth is not noticeable unless the diameter of the chosen section is well below

(<80%) the true particle diameter. Since the average particle diameter of ECR1030M and ECR8204M is approx. 500 µm, only sections with a diameter larger than 400 µm were used for this study.

Table S1. Influence of cutting height on apparent penetration depth and section diameter. $l_{Enzyme,\ eq}$ is the true enzyme penetration depth.

Visual representation of cutting plane	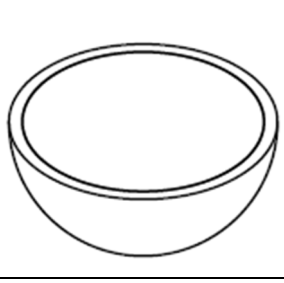	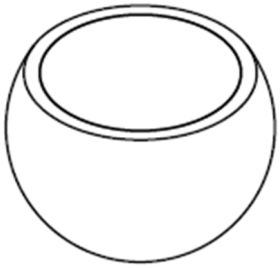	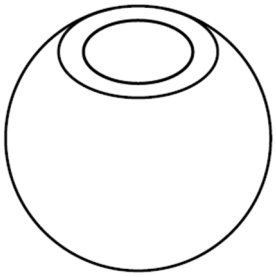
Section diameter	$r_{Section} = r_{Particle}$	$r_{Section} = r_{Particle} \cdot 80\%$	$r_{Section} = r_{Particle} \cdot 60\%$
Section diameter	500 µm	400 µm	300 µm
Penetration depth	$l_{Enzyme} = l_{Enzyme,\ eq} \cdot 100\%$	$l_{Enzyme} = l_{Enzyme,\ eq} \cdot 129\%$	$l_{Enzyme} = l_{Enzyme,\ eq} \cdot 188\%$
Penetration depth	25 µm	32 µm	47 µm

5. Repeat measurements

Five independent sections of ECR1030M after 1 h of immobilization were examined with IR microscopy to assess the repeatability of the measurement. The absolute penetration, as measured by IR microscopy and averaged over the left and right border of the particle, is depicted in Figure S8. Over the five independent samples, an average of 37 µm with a 1 σ standard deviation of 5 µm was found for the 1 h time point.

Considering the good reproducibility of the IR microscopic measurement, single determinations were deemed sufficient for this study.

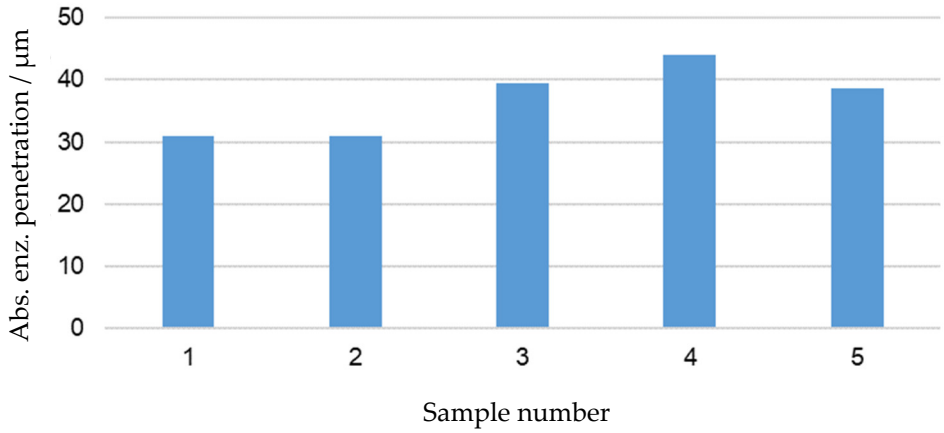

Figure S8. Absolute enzyme penetration of five repeat measurements of independent sections of ECR1030M after 1 h of immobilization.